



# The decomposition of 2-pentyl and 3-pentyl radicals

Jeffrey A. Manion<sup>\*</sup>, Iftikhar A. Awan

*Chemical and Biochemical Reference Data Division, National Institute of Standards and Technology, Gaithersburg, MD 20899-8320, United States*

Available online 15 July 2012

## Abstract

The isomerization and decomposition reactions of 2-pentyl and 3-pentyl radicals have been studied in a single-pulse shock tube over a temperature range of 973–1121 K and pressures of 120–800 kPa. The results represent the first direct study of the alkene product branching ratio resulting from the kinetics of the competition between isomerization and beta C–C bond scission for a secondary straight-chain alkyl radical at high temperatures. Such species are representative of intermediates important in the combustion of typical hydrocarbon fuels. In the present work, a small quantity of precursor ( $\sim 45 \mu\text{L/L}$ ) is used to thermally generate H atoms in the presence of excess (*E*)-2-pentene, leading to the radicals of interest via addition of H to the double bond. Decomposition of the chemically activated pentyl radicals results in the stable olefin products ethene, propene, and 1-butene, which are detected in postshock gas chromatographic analyses utilizing flame-ionization and mass-spectrometric detection. It is shown that the olefin product ratios can be related to the isomerization and decomposition reactions of the 2-pentyl and 3-pentyl radicals and the results are consistent with the existence of distinct non-overlapping cracking patterns for the two radicals. The data are compared with predictions made on the basis of a model developed from experiments on the decomposition of thermal (i.e. not chemically activated) 1-pentyl radicals. Good agreement is observed. In conjunction with an RRKM/Master Equation analysis, the results for 2-pentyl and 3-pentyl radicals are projected over a wide range of temperatures. In addition, the rate constants for addition of H atoms to the alternate double bond positions of (*E*)-2-pentene are derived relative to a standard reaction and absolute rate constants for these processes are reported.

Published by Elsevier Inc. on behalf of The Combustion Institute.

*Keywords:* 2-Pentyl; 3-Pentyl; Kinetics; H-atoms; (*E*)-2-pentene

## 1. Introduction

Alkyl radicals are prominent species formed during the combustion of hydrocarbon fuels and their unimolecular decomposition reactions compete with bimolecular oxidation steps. Under many conditions the unimolecular processes are

the main initial reactions. The pyrolysis steps involve isomerization reactions and the formation of olefins and smaller alkyl radicals via beta bond scission reactions. The cracking pattern of the parent radical is a primary determinant of the subsequent behavior of the system: it influences both the course of oxidation and the formation of unwanted byproducts such as soot. Reliable kinetic data and an understanding of the decomposition mechanisms is required to develop accurate simulation based engineering models used in combustion energy science [1–3].

<sup>\*</sup> Corresponding author. Fax: +1 (301) 869 4020.

*E-mail address:* [jeffrey.manion@nist.gov](mailto:jeffrey.manion@nist.gov) (J.A. Manion).

In previous work we have examined the decomposition of a number of 1-alkyl radicals [4–6] and have carried out Rice Ramsberger Kassel Marcus/Master Equation (RRKM/ME) analyses to fit the data and project the results over the pressure and temperature conditions of interest to combustion energy scientists. The RRKM/ME analyses require the construction of potential energy surfaces (PES) for the decomposition reactions, and these typically involve a number of competing channels with similar barriers. The quality of the model, and hence the accuracy of the kinetic extrapolations, can be improved if one is able to enter the system from multiple positions on the PES.

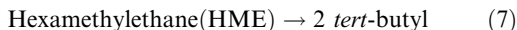
We have recently investigated the decomposition and isomerization reactions of the 1-pentyl radical at temperatures near 1000 K and pressures between 80 and 5000 kPa [7,8]. The present work represents an effort to confirm the results by entering the  $C_5H_{11}$  system from the side of the secondary alkyl radicals. There appear to be no previous experimental studies that directly probe the decomposition pattern of non-cyclic secondary alkyl radicals at high temperatures.

## 2. Experimental procedures [9]

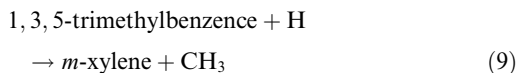
A heated single pulse shock tube has been used to carry out the experiments. Earlier publications [6,10] describe the instrument and general analytical procedures in detail. Experimental temperatures ranged from 973 to 1121 K and shock pressures were 120–800 kPa. Heating times, as derived from recorded pressure traces, were  $500 \pm 50 \mu s$ .

To generate the pentyl radicals of interest, we place a small amount (typically  $45 \mu L/L$ ) of a hydrogen atom precursor in the presence of a large excess ( $5000 \mu L/L$ ) of (E)-2-pentene. Hydrogen atoms add rapidly to the double bond, forming either the 2-pentyl or the 3-pentyl radical, depending on the site of addition. Reactions (1)–(6) in Scheme 1 summarize the postulated chemistry, and lead to ethene, propene and 1-butene as stable olefin products. Products that may be uniquely identified with specific precursor radicals are enclosed in boxes. A key point is that the product spectrums from 2-pentyl and 3-pentyl radicals are distinct and do not overlap. This will be justified later, but is a consequence of the slowness of the isomerization of 3-pentyl radical, so that this species undergoes only beta scission of the  $CH_3$  group under our conditions. Also note that the radical intermediates decompose on the time scale of a few microseconds or less, even at the lowest temperatures of our studies. The concentrations of the main products can thus not be significantly affected by the small fraction of radicals that survive until the postshock quenching period.

We form the necessary hydrogen atoms by the thermal decomposition of hexamethylethane (HME), reactions 7 and 8, a technique used in this laboratory for many years [11]:



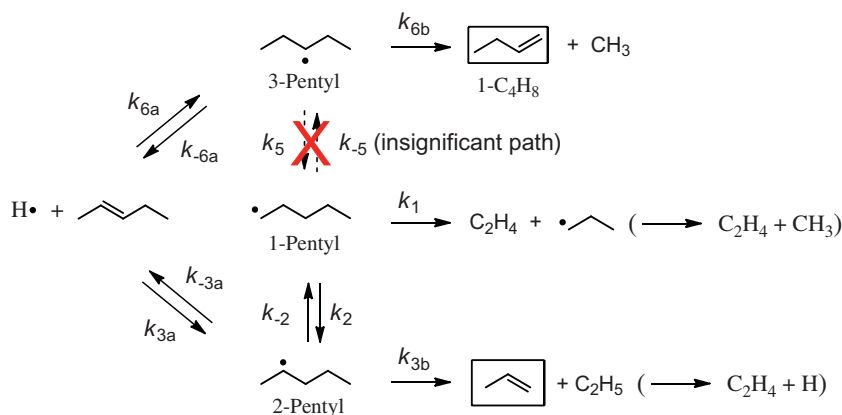
Chain processes are controlled by the addition of about  $5000 \mu L/L$  of the free radical scavenger 1,3,5-trimethylbenzene (135TMB). Some H atoms are lost by reaction with 135TMB, either via abstraction of H to give the unreactive 3,5-dimethylbenzyl radical (DMB), or displacement of methyl from the ring to produce m-xylene:



Methyl radicals produced above can similarly abstract H from 135TMB. H atoms and methyl radicals can also abstract H from 2-pentene. These reactions and the recombination processes of stabilized radicals lead to some secondary products that will be discussed subsequently, but this chemistry will be shown to have no impact on the C2–C4 olefins of primary interest.

Product analysis employs an Agilent Technologies 6890N gas chromatograph (GC) equipped with a J & W Scientific DB-1  $30 \text{ m} \times 0.53 \text{ mm}$  internal diameter (i.d.) fused silica capillary column for the larger species and a Restek  $30 \text{ m} \times 0.53 \text{ mm}$  i.d. Rt–Alumina (aluminum oxide porous layer) capillary column for the lighter components. The GC is equipped with both flame ionization detection (FID) and an Agilent Technologies 5973 Inert mass selective detector. The sample eluting from the DB-1 column was split for simultaneous identification and quantification of the mixture components by mass spectrometry and FID analysis. The GC oven temperature was programmed from  $-60 \text{ }^\circ\text{C}$  to  $180 \text{ }^\circ\text{C}$ .

Shock temperatures are determined by following the progression of a standard reaction with a known rate constant. At temperatures above 1020 K we utilized the decomposition of HME as our temperature standard, using the known [12,13] rate expression  $k(\text{HME} \rightarrow 2\text{-t-butyl}) = 10^{15.4} \exp(-31100/T) \text{ s}^{-1}$ . At temperatures lower than 1020 K we employed the decomposition of chlorocyclopentane. This standard is more accurate than HME at lower temperatures where conversion of HME is very low. It additionally provides a direct comparison with results from our study of 1-pentyl radical, where it was also used. The rate expression  $k(\text{chlorocyclopentane} \rightarrow \text{cyclopentene} + \text{HCl}) = 10^{15.4} \exp(-31100/T) \text{ s}^{-1}$  is from our recent comprehensive study [14] and critical evaluation of several temperature standards. Around 1020 K, where both standards should be



Scheme 1.

accurate, derived temperatures agreed within 4 K. Shock pressures were calculated from the temperature and mixture composition via the ideal shock equations. These were in good agreement with less precise values derivable from the pressure traces.

Chemicals used were (*E*)-2-pentene (99.9%, Aldrich), 135TMB (99%, Aldrich), hexamethylethane (98%, Aldrich), chlorocyclopentane (99%, Aldrich), and high-purity Argon (Praxair, 99.999%). Primary impurities in 135TMB and (*E*)-2-pentene were other trimethylbenzene isomers in the former case and 0.097% (*Z*)-2-pentene in the latter. 135TMB was distilled prior to use, reducing the *m*-xylene impurity to <0.1  $\mu$ L/L. Chemicals were degassed during preparation of the mixtures. Two mixtures were utilized, the first containing of 4080  $\mu$ L/L (*E*)-2-pentene, 5900  $\mu$ L/L 135TMB, 46  $\mu$ L/L hexamethylethane, and 75  $\mu$ L/L chlorocyclopentane in argon; the second was comprised of 6230  $\mu$ L/L (*E*)-2-pentene, 3940  $\mu$ L/L 135TMB, 45  $\mu$ L/L hexamethylethane, and 75  $\mu$ L/L chlorocyclopentane, also in argon.

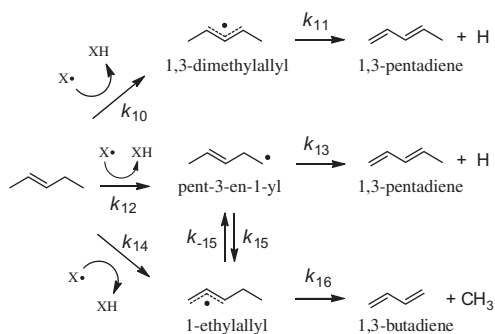
FID responses of all major olefin products were determined from standard samples. Peak areas from the standards are reproducible typically within 2–3% and overall standard uncertainties ( $1\sigma$ ) are estimated at about 5%. Values for some minor products having no direct impact on our kinetic analysis were estimated based on carbon number and standard FID response relationships. These should have standard uncertainties of about 8%. Peak areas were determined using the HP ChemStation software.

### 3. Results and discussion

#### 3.1. Products and mechanism

Product data from individual experiments are provided in [Supplementary Table S1](#). Ethene, propene, 1-butene, isobutene, 1,3-butadiene, 1,3-

pentadiene, and cyclopentene are the major olefinic products. We also find a quantity of *m*-xylene. *m*-Xylene results from H atom attack on our inhibitor, reaction 9. Isobutene stems from our H atom source, and cyclopentene from our temperature standard. The other olefins are attributed to radical attack on (*E*)-2-pentene. Products from addition of H to (*E*)-2-pentene are delineated in [Scheme 1](#). Radicals may also abstract H from (*E*)-2-pentene, however, resulting in a different set of reactions. The main paths are indicated as reactions (10)–(16) in [Scheme 2](#) and account for the observed 1,3-butadiene and 1,3-pentadiene. 1,3-Butadiene is formed in amounts roughly three times that of 1,3-pentadiene. This ratio may reflect several factors, including the number of abstractable hydrogens that lead to the precursor radicals, the interconversion of the precursors, and the lower stability of the 1-ethylallyl radical (pent-2-en-1-yl) in comparison with 1,3-dimethylallyl (pent-3-en-2-yl), due to the more facile C–C bond scission decomposition path that is available in the former case. With respect to isomerization of the alkenyl precursors shown in [Scheme 2](#), a



Scheme 2.

detailed understanding of the effect of the double bond on intramolecular H transfer does not yet exist, but the most facile reaction is undoubtedly the six-center 1–5 H shift reaction that converts pent-3-en-1-yl to 1-ethylallyl. The other possible H-shifts (not shown) involve highly strained and thermodynamically disfavored reactions. The chemistry shown in Scheme 2 leads to the release of methyl radicals into the system, as well as a quantity of H atoms above that directly generated by decomposition of HME. The abstracting radicals, X, indicated in Scheme 2 are undefined but are expected to be predominantly H atoms and methyl radicals. There is no way of distinguishing the abstracting radical, however, so we are unable to determine kinetic parameters on the basis of these data. For our purposes, the important feature is that the abstraction channels do not result in the same products as those that are associated with the decomposition of 2-pentyl and 3-pentyl radicals (Scheme 1).

### 3.1.1. Secondary chemistry

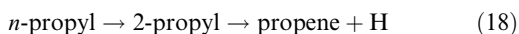
Aside from the species noted above, methane, ethane and 3,5-dimethylethylbenzene were the only other species identified in relatively large amounts. Methane and ethane stem from methyl radicals via ( $\text{CH}_3 + \text{RH} \rightarrow \text{CH}_4 + \text{R}$ ) and ( $\text{CH}_3 + \text{CH}_3 \rightarrow \text{C}_2\text{H}_6$ ). Note that the chemically activated process ( $\text{CH}_3 + \text{CH}_3 \rightarrow \text{C}_2\text{H}_5 + \text{H}$ ), which could impact ethene yields, is insignificant under our conditions [15] (calculated corrections, Table S1, are 0.05–0.5%). Abstraction of H from the methyl groups of the 135TMB inhibitor leads to the resonance stabilized 3,5-dimethylbenzyl radical (DMB), which recombines with methyl and accounts for the 3,5-dimethylethylbenzene. The C18 species resulting from  $\text{DMB} + \text{DMB}$  is presumably formed but does not elute from the GC column under our conditions. Aside from methyl and DMB, the most stable radicals in the system are the substituted allyl radicals noted in Scheme 2. Although these have unimolecular modes of decomposition, we were able to identify small amounts of the C6 olefins resulting from the recombination of these species with methyl radicals. The analogous C15 products expected from reaction with DMB do not elute under our conditions.

The high sensitivity of GC/MS analysis allows us to identify a variety of other trace products at levels of 0.05–1% of the amounts of the olefin products of interest. Observed products are predominantly those expected from radical recombination reactions of trace alkyl radicals. Quantities are not large enough to significantly affect our results, so we refrain from detailed discussion in the present report.

Pent-3-en-1-yl, produced by abstraction of H from (*E*)-2-pentene (Scheme 2), is postulated to

isomerize to 1-ethylallyl (leading to 1,3-butadiene and  $\text{CH}_3$ ) or decompose directly to 1,3-pentadiene and an H atom. An alternate channel of potential interest involves beta C–C scission to form ethene and 1-propenyl. If significant, this could impact our ethene yields. However, previous work,[16,17] shows that 1-propenyl will rapidly eject methyl and the net process will be ( $\text{pent-3-en-1-yl} \rightarrow \text{ethene} + \text{ethyne} + \text{CH}_3$ ). Ethyne is stable under our conditions and was largely absent from the product spectrum, reaching a maximum level of about 2% of ethene at the highest temperatures. On this basis the above channel may be neglected.

In Scheme 1 we assume that *n*-propyl radicals decompose exclusively to give ethene and a methyl radical. Alternate channels that could impact our conclusions involve direct or indirect ejection of H to form propene:



An exact measurement of the branching ratio to propene and H is not available. The most direct information comes from the work of Yamauchi et al. [18] who used atomic resonance absorption spectroscopy (ARAS) to measure H atom yields for a series of alkyl radicals between 950 and 1400 K. For *n*-propyl they determined a maximum branching fraction of 0.03–0.05 for H atom formation, and suggested that even this value could be too high due to impurities in their system. Less directly, product data from our previous work [7] show that  $\beta$ -scission of C–H in 2-pentyl to give 2-pentenenes accounts for <0.4% of reaction. In our previous RRKM/ME analysis of the decomposition of 1-pentyl radicals we also tested the possible contribution of three-center 1–2 H shift reactions (analogous to reaction 18), which theory suggests have barriers of near 170 kJ/mol.[19] The computed contribution was <1%. Our observations on 1-pentyl are not directly transferrable, but if one accounts for differences in thermochemistry and rates of methyl vs. *n*-alkyl scission, the conclusion is that the branching fraction of *n*-propyl to propene + H is a few percent or less under the present conditions. As discussed in Section 3.4, this has little impact on the net propene/ethene ratio.

2-Pentene itself is expected to be thermally stable under our conditions on the basis of rate constants measured for related compounds [20], and confirmed in the present experiments by the absence of noticeable loss of the starting substrate. Any trace decomposition would be through fission of the relatively weak allylic C–C bond, leading to  $\text{CH}_3$  and 1-methylallyl radical (but-2-en-1-yl). While the latter species could be a source of butadiene through beta scission of H, there are no expected pathways that would impact ethene and propene, the olefins of primary interest.

We make one minor correction to the propene yield as a result of the chemistry of our H atom source, hexamethylethane (HME). Tsang has observed that decomposition of HME gives a propene/isobutene product branching ratio of 0.03 [21]. The branching ratio under the present temperature and pressure conditions was confirmed to be  $0.03 \pm 0.005$  in separate experiments with mixtures containing only HME, 135TMB, and argon. The source of propene is not completely clear: it may be due to a *I*-2 H atom shift in the *t*-butyl radical formed in reaction 7, followed by ejection of methyl; an alternative is direct formation from HME in a “roaming” reaction of the type postulated by Harding and Klippenstein.[22] Mechanism aside, the reaction necessitates that propene yields are reduced by an amount equal to 0.03[isobutene]. This typically leads to a correction (Table S1) of about 2%.

### 3.2. Kinetics of H atom addition and isomerization of (*E*)-2-pentene

Although not the main focus of the present study, we are able to derive rate parameters for attack of H atoms on the double bond of (*E*)-2-pentene. As shown in Scheme 1, addition of H may occur at either the 2 or the 3 position, resulting in 3-pentyl and 2-pentyl, respectively. The 2-pentyl radical can isomerize to the 1-pentyl radical via a relatively facile 2,5 H shift, a five center process, whereas isomerization of 3-pentyl requires either a 3-1 or a 3-2 H shift, which are highly strained four-center and three-center processes, respectively. Our recent study of the decomposition products of 1-pentyl radicals [7] shows that <0.5% of the product spectrum is accounted for by the *I*-3 H transfer reaction (1-pentyl  $\rightarrow$  3-pentyl). The reverse 3-1 process, of potential interest in the present system, is endothermic and therefore even slower. The data on 1-pentyl show that three-center H shifts are likewise very slow relative to decomposition via beta C-C scission. These results are in agreement with theory [19] and our RRKM/ME analysis presented later. Consequently, we may conclude that 1-butene is formed essentially exclusively via addition of H to give the 3-pentyl radical, whereas the propene and ethene yields pertain to the alternate site. Upon addition of H, the subsequent decomposition of 2-pentyl and 3-pentyl radicals via C-C bond scission reactions is very much faster than reversal of H atom addition under our conditions. Experimentally, we are nearly blind to re-ejection of H since it changes the product spectrum only by conversion of some fraction of the starting (*E*)-2-pentene to (*Z*)-2-pentene, or by formation of 1-pentene from the 2-pentyl radical. We were unable to accurately measure the expected trace levels of 1-pentene due to a background of this compound. Although we observe the formation of a small amount of

(*Z*)-2-pentene ( $\leq 2\%$  of (*E*)-2-pentene, Table S1), the (*E*) to (*Z*) conversion also occurs in a unimolecular process that, although relatively slow, is expected to overwhelm the radical-induced chemistry. If we assume a purely unimolecular basis, our data lead to:

$$\begin{aligned} k[(E)\text{-}2\text{-pentene} \rightarrow (Z)\text{-}2\text{-pentene}]/s^{-1} \\ = 10^{(13.83 \pm 0.20)} \exp\{(-31582 \\ \pm 492)K/T\}; (1001\text{--}1121) \text{ K}; 120\text{--}800 \text{ kPa} \end{aligned}$$

The listed uncertainty is  $1\sigma$  and is precision only. Derived rate constants are about 20% smaller than those reported by Jeffers [23] for the [(*Z*)-2-butene  $\rightarrow$  (*E*)-2-butene] reaction. The slightly smaller rate constant for the present case is consistent with the small endothermicity associated with the (*E*) to (*Z*) process.

Returning to the decomposition of 2-pentyl and 3-pentyl radicals via re-ejection of H, our RRKM/ME model presented later suggests that this path is only a few percent. As a result, C2-C4 olefin product amounts correspond closely with rates of H atom addition. Consequently, the molar product yields can be related to the relative rate constants for H atom addition by:

$$\frac{k_{6a}}{k_{3a}} \approx \frac{[1\text{-butene}]}{[\text{propene}] + 0.5([\text{ethene}] - [\text{propene}])} \quad (19)$$

These data are plotted in Fig. 1, and lead to:

$$\begin{aligned} \frac{k_{3a}}{k_{6a}} \approx 10^{(0.044 \pm 0.039)} \exp\{-(26 \\ \pm 94) K/T\}; 973\text{--}1121 \text{ K}; 120\text{--}800 \text{ kPa}, \end{aligned} \quad (20)$$

where the uncertainty is  $1\sigma$  and is precision only. There is no discernible variation of the ratio with pressure or temperature: the data could also be represented as  $k_{3a}/k_{6a} = 1.08 \pm 0.08$ , where the

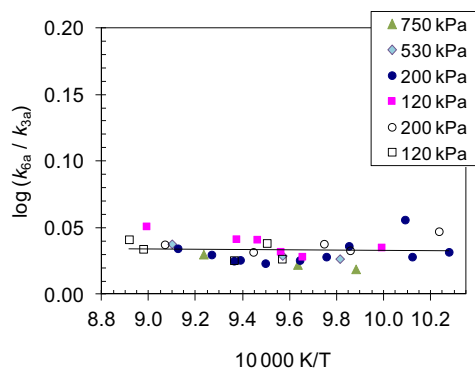


Fig. 1. Relative rates of H atom attack on the alternative double bond positions of (*E*)-2-pentene (see Scheme 1). Filled symbols refer to mixture 1 and unfilled to mixture 2; approximate pressures are given in the legend.



indicated uncertainty includes estimates for both analytical and systematic effects.

In a similar fashion we can determine rate constants for H atom attack on (*E*)-2-pentene relative to  $k_9$ , the displacement of methyl from 1,3,5-trimethylbenzene. Noting that amounts of (*E*)-2-pentene and 1,3,5-trimethylbenzene are essentially unchanged during reaction, the equations are:

$$\frac{k_9}{k_{3a}} \approx \frac{[m\text{-xylene}]}{[\text{propene}] + 0.5([\text{ethene}] - [\text{propene}])} \times \frac{[E\text{-}2\text{-pentene}]_0}{[1, 3, 5\text{-trimethylbenzene}]_0} \quad (21)$$

$$\frac{k_9}{k_6} = \frac{[m\text{-xylene}]}{[1\text{-butene}]} \frac{[E\text{-}2\text{-pentene}]_0}{[1, 3, 5\text{-trimethylbenzene}]_0} \approx \frac{k_9}{k_{6a}} \quad (22)$$

The results for  $k_9/k_6$  are plotted in Fig. 2. There is a small systematic difference of about 8% in the results for the two mixtures. Since the relative amounts of ethene, propene, and 1-butene are the same in both mixtures (Fig. 1), this does not appear to be due to an extraneous source of one of the C2–C4 olefins. It is difficult to imagine an alternate source of *m*-xylene, so the apparent difference probably reflects uncertainties in the (*E*)-2-pentene/1,3,5-trimethylbenzene ratios. The size of discrepancy is not unreasonable, given analytical precisions of about 5% for each component. Averaging the results for the two mixtures we obtain:

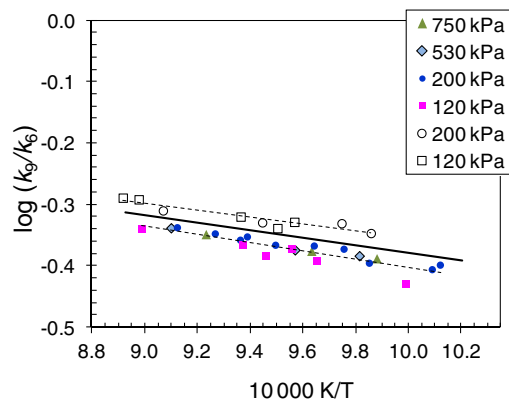


Fig. 2. Relative rate constants for H atom displacement of methyl from 1,3,5-trimethylbenzene vs. displacement of methyl from (*E*)-2-pentene. Filled symbols refer to Mixture 1 and unfilled to Mixture 2; approximate pressures are given in the legend. Dashed lines indicate least-squares results for the individual mixtures and the solid line is the value recommended in the text based on all data.

$$\frac{k_9}{k_6} \approx \frac{k_9}{k_{6a}} = 1.74 \exp(-1429 \text{ K}/T) \quad (23)$$

And, combined with the data of Fig. 1,

$$\frac{k_9}{k_{3a}} \approx 1.93 \exp(-1455 \text{ K}/T) \quad (24)$$

Based on our experimental technique and analytical uncertainties, the standard uncertainties ( $1\sigma$ ) in the above relative rates and relative activation energies should be about  $\pm 10\%$  and 360 K ( $3 \text{ kJ mol}^{-1}$ ). Relative to the standard reaction of displacement of methyl from 135TMB, for which  $k_9 = 6.7 \times 10^{13} \exp(-3255 \text{ K}/T) \text{ cm}^3 \text{ mol}^{-1} \text{ s}^{-1}$ , [12,13] we arrive at:

$$k_{3a}/\text{cm}^3 \text{ mol}^{-1} \text{ s}^{-1} \approx 4.26 \times 10^{13} \times \exp(-1853 \text{ K}/T); 942\text{--}1075 \text{ K} \quad (25)$$

$$k_6/\text{cm}^3 \text{ mol}^{-1} \text{ s}^{-1} \approx k_{6a} = 3.84 \times 10^{13} \times \exp(-1826 \text{ K}/T); 942\text{--}1075 \text{ K} \quad (26)$$

Standard uncertainties in the absolute rate constants and activation energies are estimated at about 30% and  $5 \text{ kJ mol}^{-1}$ , respectively. The values of  $k_6$  and  $k_{3a}$  at 1050 K are respectively 2% and 10% larger than the rate constant measured for displacement of methyl from propene using the same technique [24].

### 3.3. Kinetic models for chemically activated decomposition of 2-pentyl and 3-pentyl radicals

The decompositions under consideration involve multiple bond scission channels, pressure dependent rate constants, and isomerization reactions that are reversible. It is necessary to employ a detailed model and a Rice Ramsberger Kassel Marcus/Master Equation (RRKM/ME) analysis to fit the data. In the case of the cyclopentyl  $\rightleftharpoons$  1-pentenyl system [25] experiments showed significant inconsistencies in models developed solely on the basis of theory or data obtained by entering the system from one side of the reaction. Possible models were much better constrained after consideration of kinetic data pertaining to multiple positions of the PES. An important aim of the present work is to further test our recently developed model for the decomposition of 1-pentyl radicals. This model is based on shock tube measurements of experimental product branching ratios obtained in the thermal decomposition of 1-pentyl radicals near 950 K [7,8]. The potential energy surface (PES) has been developed using quantum chemical calculations and then critically adjusted so as to match the pressure-dependent product branching ratios and relevant kinetic data from experiments at lower temperatures. Structural properties (geometries, vibrational frequencies, internal and external moments of inertias) for the radicals and stable species in the model

are based on computations at the G3MP2B3 level of theory. Computed frequencies are scaled by 0.96. Thermodynamic parameters are then derived using a modified Rigid Rotator Harmonic Oscillator (RRHO) treatment in which the modes corresponding to internal rotations are approximated with symmetric  $n$ -fold potentials using the methodology of Pitzer[26]. Energy transfer is treated with a standard exponential-down model.[27–30] The energy transfer parameter was taken as  $\langle \Delta E_{\text{down}} \rangle / \text{cm}^{-1} \text{K}^{-1} = 0.675T$ , where  $T$  is in Kelvin, in order to match the experimental pressure dependence observed in 1-pentyl decomposition. More details can be found in the previous publications [7,8].

### 3.4. Comparisons of the model with experiment

The present study employs the potential energy surface developed in our previous works [7,8] and RRKM/ME calculations are carried out with the ChemRate software package [31,32]. The only adjustments to the previous model are changes in the starting radical isomer and a change from a thermal energy distribution to one that is augmented by roughly  $145 \text{ kJ mol}^{-1}$  of energy due to the exothermicity of H atom addition. In ChemRate this is accomplished by specifying the reaction that creates the starting radical, so that we automatically account for the temperature dependence of the chemical activation energy. Figure 3 compares propene/ethene ratios computed for the decomposition of chemically activated 2-pentyl radical with values from the present experiments. Predicted values are about 0.89 whereas the observed values are about 0.80. The difference could indicate an imbalance in the relative rates of the beta C–C bond scission and 2-5 H transfer reaction in the 2-pentyl radical. The results agree, however, within the overall uncertainty in the experimental branching ratio, which, including systematic errors, is estimated at about 12% at the  $2\sigma$  level of confidence. The lack of a significant pressure effect is in good agreement with the experimental observations, as is the predicted temperature dependence. In the above comparison we assume that the experimentally observed ethene and propene stem solely from decomposition of the 2-pentyl radical, with no contribution from 3-pentyl. Computed product branching ratios for the two C5 radicals are shown in Figs. 4 and 5. For completeness, these calculations include estimates for very minor beta C–H bond scission channels, but these reactions play no significant role in product formation. Under our conditions, computed ethene/1-butene values derived for the decomposition of 3-pentyl radical are about 0.01 whereas propene/1-butene values are about 0.001. Inclusion of the very minor contribution from 3-pentyl would slightly lower the predicted propene/ethene ratio to a

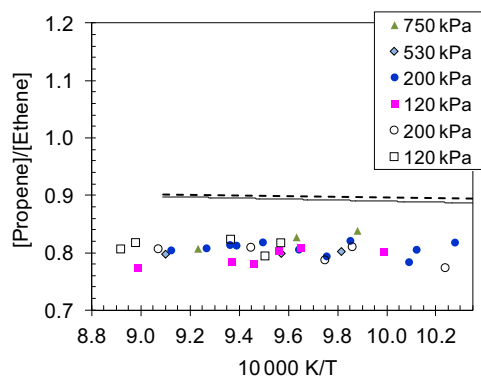


Fig. 3. Propene/Ethene ratios in the decomposition of chemically activated 2-pentyl radicals formed by addition of H to (*E*)-2-pentene. Symbols represent experimental data at the indicated pressures. Dashed and solid lines represent the results at 120 kPa and 750 kPa, respectively, of an RRKM/Master Equation analysis using the using our “best fit” model [7,8], which was developed from studies of the decomposition of thermal 1-pentyl radicals.

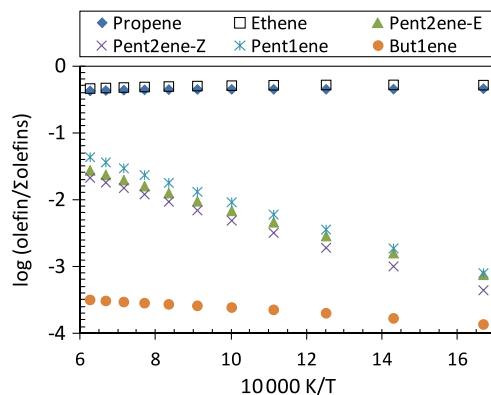


Fig. 4. Computed high pressure limiting product branching ratios in the decomposition of chemically activated 2-pentyl radicals formed by addition of H to (*E*)-2-pentene.

value of about 0.88. As noted earlier, our simplified mechanism (Scheme 1) does not include any possible contribution to propene from C–H bond scission in 1-propyl radicals. Under our conditions, our best current estimate (Section 3.1) is that the branching fraction to propene + H is  $\leq 0.02$ , with a maximum possible value of about 0.05. Unless grossly incorrect, this estimate has little impact on our conclusions. This is because by far the main source of propene is the 2-pentyl radical, and the product spectrum dictates that 2-pentyl is present at roughly ten times the concentration of the 1-pentyl radical under all conditions. If even 10% of the 1-propyl radicals

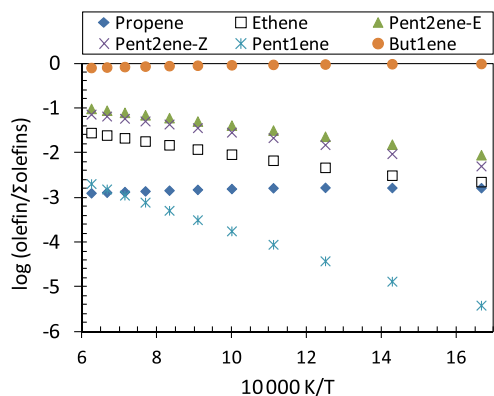


Fig. 5. Computed high pressure limiting product branching ratios in the decomposition of chemically activated 3-pentyl radicals formed by addition of H to (*E*)-2-pentene.

that are derived from 1-pentyl were to decompose to propene + H, the overall propene/ethene ratio would increase by less than 0.01.

Finally, notice that the data presented in Figs. 4 and 5 show that the C2–C4 product spectrums of 2-pentyl and 3-pentyl radicals do not significantly overlap, thereby confirming the validity of the kinetic treatment presented in Section 3.2.

To aid chemical kinetic modeling, in the supplementary material we provide high pressure limiting rate expressions, pressure dependent rate expressions covering 600 – 1700 K and 10 – 100 000 kPa in the PLOG format used by ChemKin Pro, and thermodynamic parameters of the model species in NASA polynomial format.

#### 4. Conclusions and implications for combustion modeling

Product branching ratios have been determined for the decomposition of chemically activated 2-pentyl and 3-pentyl radicals. The results represent the first direct study of the kinetics of the competition between isomerization and beta C–C bond scission for secondary straight-chain alkyl radicals at high temperatures. At temperatures near 1000 K nearly all 3-pentyl radicals decompose to 1-butene and methyl radical whereas the 2-pentyl radical undergoes partial isomerization and produces a propene/ethene ratio of  $0.80 \pm 0.10$ . Product branching ratios are nearly unchanged over the studied temperature and pressure ranges of 975–1120 K and 120–800 kPa. Although a small discrepancy remains, predictions made on the basis of a model created to describe the decomposition of thermal 1-pentyl radicals agree with the experimental results within the uncertainty bounds.

Compared with the 1-pentyl radical [7,8], the temperature and pressure dependence of the prod-

uct branching ratio is much weaker for 2-pentyl and 3-pentyl radicals. In part this is due to the shift in the thermochemistry of the isomerization reactions from exothermic to endothermic. This makes isomerization less competitive with beta bond scission reactions and reduces the relative importance of the former process. When starting with chemically activated 2-pentyl radical, the present results show that under our conditions only about (8–10)% of the olefin products are derived from the 1-pentyl radical formed by the 2-5 H shift reaction. When starting with chemically activated 3-pentyl radical, isomerization results in only about 1% of the products. Cracking patterns of the three isomeric pentyl radicals are distinct despite the influence of intramolecular H transfer reactions. The relatively small contribution of isomerization in the present case is not necessarily a general feature of secondary alkyl radical chemistry. As one moves to systems larger than C5 the much more facile six-center H shift reactions will become available and thermoneutral secondary to secondary processes will also become possible. This will significantly increase the role of isomerization.

#### Appendix A. Supplementary data

Supplementary data associated with this article can be found, in the online version, at <http://dx.doi.org/10.1016/j.proci.2012.05.078>.

#### References

- [1] M. Colket, T. Edwards, S. Williams et al., in: AIAA paper, AIAA-2007-770, 2007.
- [2] J.T. Farrell, N.P. Cernansky, F.L. Dryer et al., in: SAE Paper, SAE 2007-01-0201, 2007.
- [3] H. Richter, J.B. Howard, *Prog. Energy. Combust.* 4 (2000) 565–608.
- [4] W. Tsang, J.A. Walker, J.A. Manion, *Proc. Combust. Inst.* 31 (2007) 141–148.
- [5] W. Tsang, W.S. McGivern, J.A. Manion, *Proc. Combust. Inst.* 32 (2009) 131–138.
- [6] I.A. Awan, W.S. McGivern, W. Tsang, J.A. Manion, *J. Phys. Chem. A* 114 (30) (2010) 7832–7846.
- [7] I.A. Awan, D.R. Burgess Jr., J.A. Manion, *J. Phys. Chem. A* 116 (2012) 2895–2910.
- [8] A. Comandini, I.A. Awan, J.A. Manion, *Chem. Phys. Lett.*, submitted for publication.
- [9] Disclaimer, Certain commercial materials and equipment are identified in this paper in order to specify adequately the experimental procedure. In no case does such identification imply recommendation of endorsement by the National Institute of Standards and Technology, nor does it imply that the material or equipment is necessarily the best available for the purpose.
- [10] W.S. McGivern, I.A. Awan, W. Tsang, J.A. Manion, *J. Phys. Chem. A* 112 (30) (2008) 6908–6917.
- [11] J.A. Manion, W. Tsang, *J. Phys. Chem.* 100 (17) (1996) 7060–7065.



- [12] W. Tsang, J.P. Cui, J.A. Walker, in: *Proceedings of the 17th International Symposium on Shock Waves & Shock Tubes, Bethlehem PA AIP Conference Proceedings 208*, American Institute of Physics, Melville NY, 1990, vol. 208, pp. 63–73, <http://dx.doi.org/10.1063/1.39497>.
- [13] J.A. Manion, R.E. Huie, R.D. Levin et al., NIST Chemical Kinetics Database NIST Standard Reference Database 17, Version 7.0 (Web Version), Release 1.4.3, Data version 2011.11, National Institute of Standards and Technology, Gaithersburg, Maryland, 20899-8320, available at <http://kinetics.nist.gov/>.
- [14] I.A. Awan, D.R. Burgess Jr., W. Tsang, J.A. Manion, *Int. J. Chem. Kinet.* 44 (6) (2011) 351–368.
- [15] D.L. Baulch, C.T. Bowman, C.J. Cobos, et al., *J. Phys. Chem. Ref. Data* 34 (3) (2005) 757–1397.
- [16] J.A. Miller, J.P. Senosiain, S.J. Klippenstein, Y. Georgievskii, *J. Phys. Chem. A* 112 (39) (2008) 9429–9438.
- [17] C.M. Rosado-Reyes, J.A. Manion, W. Tsang, *J. Phys. Chem. A* 114 (18) (2010) 5710–5717.
- [18] N. Yamauchi, A. Miyoshi, K. Kosaka, M. Koshi, N. Matsui, *J. Phys. Chem. A* 103 (15) (1999) 2723–2733.
- [19] C.J. Hayes, D.R. Burgess Jr., *J. Phys. Chem. A* 113 (2009) 2473–2482.
- [20] W. Tsang, *Int. J. Chem. Kinet.* 10 (6) (1978) 599–617.
- [21] W. Tsang, *J. Chem. Phys.* 44 (11) (1966) 4283–4295.
- [22] L.B. Harding, S.J. Klippenstein, *J. Phys. Chem. Lett.* 1 (20) (2010) 3016–3020.
- [23] P.M. Jeffers, *J. Phys. Chem.* 78 (15) (1974) 1469–1472.
- [24] C.M. Rosado-Reyes, J.A. Manion, W. Tsang, *J. Phys. Chem. A* 115 (13) (2011) 2727–2734.
- [25] I.A. Awan, D.R. Burgess, W. Tsang, J.A. Manion, *Proc. Combust. Inst.* 33 (2011) 341–349.
- [26] K.S. Pitzer, *J. Chem. Phys.* 12 (1944) 310–314.
- [27] D.C. Tardy, B.S. Rabinovitch, *Chem. Rev.* 77 (3) (1977) 369–408.
- [28] D.C. Tardy, B.S. Rabinovitch, *J. Phys. Chem.* 90 (6) (1986) 1187–1193.
- [29] R.G. Gilbert, S.C. Smith, *Theory of Unimolecular and Recombination Reactions*, Blackwell Scientific Publications, Oxford, 1990.
- [30] H.H. Carstensen, A.M. Dean, in: *Comprehensive Chemical Kinetics*, R.W. Carr, (Eds.) Elsevier, Amsterdam, 2007, vol. 42, pp. 105–187.
- [31] W. Tsang, V. Bedanov, M.R. Zachariah, *J. Phys. Chem. A* 100 (1996) 4011–4018.
- [32] V. Mokrushin, W.S. McGivern, V. Bedanov et al., ChemRate, Version 1.5.6.; National Institute of Standards and Technology: Gaithersburg, Maryland, 2008.